Research Article

Received: 11 April 2022 Revised: 6 June 2022 Accepted article published: 11 June 2022 Published online in Wiley Online Library: 6 July 2022

(wileyonlinelibrary.com) DOI 10.1002/pi.6431

Free volume expansion in some polybutadiene–acrylonitrile rubbers: comparison between theory and experiments

Giovanni Consolati,[a,b*] Dario Nichetti[c] and Fiorenza Quasso[a]

Abstract

The dependence of free volume on temperature was investigated in three butadiene–acrylonitrile copolymers and in a butadiene–acrylonitrile–isoprene terpolymer, above the glass transition in order to apply the lattice-hole model. Macroscopic behaviour was highlighted by dilatometry; positron annihilation lifetime spectroscopy was used to shed light on the free volume microstructure. Coupling of the two techniques allowed us to obtain the number density of holes under specific geometrical assumptions about cavities. Comparison with the theoretical free volume fraction suggests hole shapes more similar to discs than to spheres, but with aspect ratio decreasing at increasing temperature. Such preferential growth in the radial direction is not influenced by the presence of acrylonitrile, contrarily to that recently found in butadiene–isoprene blends, where an increasing amount of isoprene makes such expansion less anisotropic.

Keywords: dilatometry; elastomers; free volume; lattice-hole theory; positron annihilation; rubbers

INTRODUCTION

Introduced for the first time by Batshinski[1] to explain the viscosity of non-associated liquids, the concept of free volume has been subsequently extended to macromolecules, in correlation with temperature and molecular dimensions, by various theories proposed starting from the 1950s.[2,3] It has been remarked that the free volume is rather ambiguously defined,[4] being based on the occupied volume, of which different definitions exist.[5] Nevertheless, it is at the base of our understanding of viscoelastic properties of polymers. In fact, it allows one to easily explain several properties such as diffusivity[6] and transport in polymeric films.[7] Among the theories which include the free volume, the Simha–Somcynsky lattice-hole model[8] has been successfully applied to more than 50 amorphous polymers and blends at equilibrium.[9]

Experimentally, it is possible to explore the free volume fraction in a polymer using positron annihilation lifetime spectroscopy (PALS), a technique based on the trapping of the unstable electron–positron system, positronium (Ps), in the free volume holes,[10-12] sometimes combined with simulations.[13] Ps may be formed when a positron injected into the polymer under study meets an electron of the medium, after suitable thermalization. The exchange repulsion between the Ps electron and the surrounding ones repels Ps from the bulk and pushes it to localize into the free volume holes.

Ps in the ground state exists as para-Ps (p-Ps, antiparallel spins) and ortho-Ps (o-Ps, parallel spins). In a vacuum, p-Ps has a lifetime of 125 ps; it annihilates in two gammas. On the other hand, the lifespan of o-Ps is 142 ns and annihilation occurs into three gammas.[14] Ortho-Ps in a hole has a more complex fate, due to interactions with the surrounding electrons in a relative singlet state, which make possible annihilation in two gammas. Such an alternative channel, called 'pickoff', depends on the electron density around Ps and may reduce its lifetime with respect to vacuum up to two orders of magnitude.

Ps is particularly suitable to probe small cavities, having the same size as hydrogen; however, it is much lighter (by a factor of about 2000). This implies that quantum effects have to be taken into consideration. Of course, a smaller cavity induces a higher annihilation probability, with consequent shortening of o-Ps lifetime. This correlation is the core of the PALS technique applied to polymers. It allows one to obtain the size of a hole from o-Ps lifetime, provided that the cavity, actually irregularly shaped, is framed in a regular geometry by means of a suitable quantum mechanical model.

Holes are generally assumed to be spherical; such a choice has the advantage of simplicity, but it does not produce necessarily

* *Correspondence to: G Consolati, Department of Aerospace Science and Technology, Politecnico di Milano, Via LaMasa 34, 20156 Milan, Italy. E-mail: giovanni.consolati@polimi.it*

a *Department of Aerospace Science and Technology, Politecnico di Milano, Milan, Italy*

b *INFN, Sezione di Milano, Milan, Italy*

c *Rheonic Lab, Castelleone, Italy*

the best results. For instance, computer simulations show that in polyethylene-like macromolecules non-spherical shapes become important with increasing free volume hole size.[15] Cigar-like holes were found in a simulation of poly(vinylmethyl ether)[16] and non-spherical shapes were considered in stiff chain polymers.[17] For a given o-Ps lifetime, alternative geometries produce different hole volumes[18] and consequently different free volume fractions.

This last is defined, following Shritawatpong *et al.*,[19] as:

$$f = \frac{N v_h}{V_{sp}} \quad (1)$$

where V_{sp} is the specific volume and N is the number density of holes with average volume v_h. To find f we need to combine PALS results with a technique able to give the specific volume such as dilatometry; we will see in the next section how to obtain also N.

In the work presented here, we focused on the behaviour of the free volume in some elastomers and their expansion with temperature, by considering three acrylonitrile–butadiene rubbers with increasing percentage of acrylonitrile, and a polyisoprene–polybutadiene–acrylonitrile terpolymer. Our interest was triggered by an investigation of *cis*-polyisoprene[19] using PALS and the spherical approximation for the free volume holes. The results well fitted the theoretical free volume fractions, but at the price of introducing a fictitious occupied volume, that is, not corresponding to the one provided by the theory. In a previous paper concerning *cis*-polyisoprene,[20] we used an occupied volume in agreement with the theory and showed that it is possible to solve this contrast by assuming cylindrical holes forming the free volume in *cis*-polyisoprene. This stimulated us to investigate the shape of the free volume holes in other rubbers and we turned to blends containing isoprene. Preliminary results for butadiene–isoprene blends[21] seem to show that, once again, a cylindrical shape allows a better fit for the free volume fraction. However, we also found the interesting result that the growth of holes with temperature seems 'anisotropic', in the sense of a higher rate of growth in the radial direction with respect to the axial direction. By increasing the percentage of isoprene, the growth tends to be more isotropic. In other words, the presence of isoprene tends to attenuate the anisotropy. The aim of the work presented here was to investigate rubbers containing butadiene, which seems responsible for the anisotropic growth of the holes. For this purpose, we studied the free volume in three butadiene–acrylonitrile copolymers with increasing percentage of acrylonitrile in order to understand whether the presence of acrylonitrile could influence the expansion of holes with temperature. The study was completed with a terpolymer containing all the 'actors' in the same percentage, that is, butadiene, acrylonitrile and isoprene.

Although we investigated specific rubbers, we point out that our procedure is valid for any kind of polymer, provided that it is amorphous and at equilibrium. Indeed, the lattice-hole model here adopted is based on these assumptions, although the theory can be extended, in principle, also to the glassy phase.[22] Furthermore, the experimental techniques used in the study can be applied to any material.

MATERIALS AND METHODS

The investigated elastomers were named R*x*. NBR is a copolymer of acrylonitrile and butadiene monomers commercially named Europrene; it was supplied by Versalis Spa (an ENI company (https://www.versalis.eni.com)).

R1: named as N1945 is NBR with 19% (w/w) of acrylonitrile.
R2: named as N3345 is NBR with 33% (w/w) of acrylonitrile.
R3: named as N4560 is NBR with 45% (w/w) of acrylonitrile monomer.
R4: Nipol® DN120, a terpolymer of IR–BR–NBR (usually named NIBR) with 33% (w/w) of acrylonitrile monomer.

NBRs are all technical polymer grades with a purity of 97.7% and the rest are volatile matter, ash, organic acid and soap. NIBR is a technical polymer grade with a purity of 97.2% and the rest are volatile matter, ash, organic acid and soap supplied by Zeon (https://www.zeon.eu). The structural formulas of NBR and NIBR are represented in Fig. 1.

Every compound was mixed with 1.2 phr of dicumyl peroxide and then mould-cured at high temperature. We used an accurately designed laboratory internal mixer to produce an amount of 800 g of each compound. A closed chamber with 'rotating kneading rotors'[23] in a type known as a Banbury mixer accomplished the mixing. The volume of the chamber was 1 L. It consisted of two tangential wing rotors, driven at 50 rpm, with a fill factor of about 0.85; ram pressure was set at 0.4 MPa. Full cooling water was applied to rotors and shell. The dispersive mixing was realized in high-shear tapering nip regions between rotor tips and mixer wall.

Raw elastomer, in chunked form, was added into the mixing chamber of the Banbury mixer and the ram put down. The batch was mixed for about 2 min until the temperature reached about 348 K. The ram was then raised up to allow the introduction of the curative ingredient (dicumyl peroxide). The ram was put down and mixing was continued for another 2 min as the temperature increased to 373 K.

The batch was dumped to a two-roll mill mixer for cooling and sheeting in a slab of 0.7 mm in thickness. Total mixing time was 4–5 min, and final stock temperature was not higher than about 383 K.

All compounds were left at room temperature for 24 h before moulding in a 0.8 MPa press. Compression moulds were in the form of two plates of 40 cm × 40 cm that were removed from the press for loading and unloading. Mould temperature was set at 443 K and controlled by the press heating system; the mould pressure was 0.5 MPa. The curing time was 20 min for all compounds.

Table 1 collects some of the thermomechanical properties of the investigated elastomers.

Thermal analysis

Thermal analysis was carried out by means of a PerkinElmer DSC 8500 differential scanning calorimeter, calibrated with high-purity indium as standard. Each sample, whose mass was about 6 mg, was encapsulated in an aluminium pan and underwent the following procedure, under nitrogen flux (30 cm^3 min^{-1}):

(1) heating from 150 to 323 K at 20 K min^{-1}
(2) isothermal treatment for 1.0 min at 323 K
(3) cooling from 323 to 150 K at 20 K min^{-1}
(4) isothermal treatment for 10.0 min at 150 K
(5) heating from 150 to 323 K at 10 K min^{-1}.

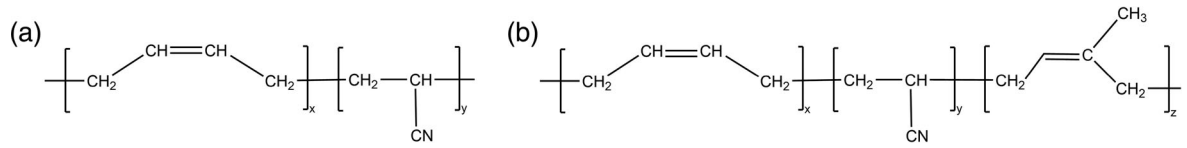

Figure 1. Structural formulas of (a) NBR and (b) NIBR.

Glass transition was evaluated from the last heating scan and the glass transition temperature (T_g) was obtained as the inflection point of the heat flow curve *versus* temperature. This was the only transition found in the temperature range explored.

Mechanical tests

The rubber hardness of cured compounds determining their resistance was measured by means of a rigid indentor under an applied force according to ISO 48.

Stress at break was measured using a Zwick tensile instrument equipped with an optical contactless extensimeter, following ISO 37. A typical tensile testing machine consists of a load cell, crosshead, extensometer, specimen grips, electronics and a drive system. It is controlled by testing software used to define machine and safety settings, and store test parameters defined by testing standards ISO 37. The amount of force applied to the machine and the elongation of the specimen are recorded throughout the test. The force required to stretch or elongate a material to the point of break is named as stress at break; it represents an ultimate property of a rubber compound.

Dynamic mechanical analysis was carried out using a TA Instruments DMA850. According to ASTM D5992, rubber samples were subjected to constant stress in a wide range of temperature between 1 and 100 Hz in order to determine the elastic plateau modulus G_e (MPa).

Positron annihilation lifetime spectroscopy

The positron source, ^{22}Na, had an activity of about 7×10^4 Bq. It was encapsulated between two Kapton® foils (thickness of 7.6 μm each), which were glued together. The whole was placed between two cylindrical samples (diameter of 2 cm), obtained from the same batch used for the dilatometric measurements. Their thickness (2 mm) ensured that all the injected positrons annihilated into the sample. The assembly was inserted inside a copper cup in contact with the heat exchanger of a liquid nitrogen cryostat (DN 1714, Oxford Instruments). The temperature controller guaranteed a stability within 0.1 K. The timing spectrometer collecting the positron spectra had a resolution of about 330 ps; it was composed of two plastic scintillators (Pilot U, 1.5-inch diameter, 1-inch height) connected to Philips XP2020 photomultipliers. A fast-fast ORTEC instrumentation completed the spectrometer. Each spectrum (containing about 10^6 counts) was analysed by means of the *LT* 9.0 computer program[24] with a suitable correction[25] (about 12%) for the positrons annihilated in the Kapton support.

Table 1. Some thermal and mechanical properties of the investigated cured elastomer compounds

	R1	R2	R3	R4
Density at 296 K (g cm^{-3})	0.96	0.97	1.01	0.99
Hardness (ShA)	41	44	53	48
T_g (K) from DSC	228	249	265	255
Stress at break (N mm^{-2})	3.20	2.88	2.30	4.40
G_e (MPa) plateau modulus	2.3	1.9	1.1	3.0

Dilatometry

Specific volume of the investigated samples was initially determined at 296 K as the inverse of the density ρ, measured by means of a Sartorius balance (model ME215P), equipped with a kit based on the buoyancy method.

Specific volume measurements as a function of the temperature were performed using a capillary dilatometer already described in previous work[26] to which we refer for details. Temperature measurements were carried out by inserting the dilatometer inside a thermostatic bath, using water (343–283 K) or ethanol (283–258 K) as circulating liquids. Minimal stability of the temperature was within 0.5 K. Three runs were carried out for each temperature. The cooling rate from a given temperature to the next one was 0.1 K min^{-1}, with a subsequent isotherm for 1000 s before starting the measurement, in order to ensure complete equilibrium.

RESULTS

The o-Ps lifetimes are shown in Fig. 2 as a function of temperature. A linear behaviour is observed with increasing temperature, which is consistent with the expansion of the cavities hosting Ps above T_g. By assuming spherical holes, we can obtain their dependence on temperature using the following Tao–Eldrup equation[27,28] between the o-Ps lifetime τ_3 and radius R of the free volume hole:

$$\tau_3 = \left\{ \lambda_t + \lambda_0 \left[1 - \frac{\Delta R}{R+\Delta R} + \frac{1}{2\pi} \operatorname{sen}\left(2\pi \frac{R}{R+\Delta R} \right) \right] \right\}^{-1} \qquad (2)$$

where $\lambda_0 \cong 2$ ns^{-1} is the annihilation rate of o-Ps in the presence of a high electron density; ΔR (= 0.166 nm) is an empirical parameter[29] accounting for the penetration of the Ps wave function into the bulk; and λ_t is the intrinsic o-Ps annihilation rate (1/142 ns^{-1}). The hole volume is calculated as $v_h = 4\pi R^3/3$.

In order to evaluate the free volume fraction (Eqn (1)), we need the dilatometric results, shown in Fig. 3. In this case, too, a linear trend with very good correlation coefficients (>0.996) is observed. These data allow us to obtain the theoretical free volume fraction h as resulting from the Simha–Somcynsky equation.[8] This last is represented, at atmospheric pressure, by the following equation:

$$\tilde{T} = 2y\left(y\tilde{V}\right)^{-2}\left[1.2045 - 1.011\left(y\tilde{V}\right)^{-2}\right]\left[1 - 2^{-1/6}y\left(y\tilde{V}\right)^{-1/3}\right] \qquad (3a)$$

Equation (3a) is coupled to a second relationship, deriving from the requirement of Helmoltz free energy minimization, which corresponds to a condition of equilibrium for the structure:

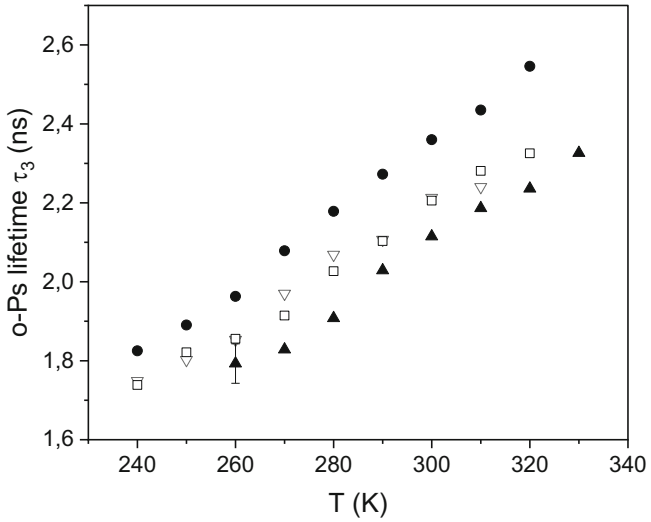

Figure 2. o-Ps lifetime *versus* temperature for the investigated elastomers (R1, circles; R2, squares; R3, down triangles; R4, up triangles). Typical uncertainty is shown only for one lifetime for the sake of clarity.

$$1+y^{-1}\ln(1-y)=\left(y/6\tilde{T}\right)\left(y\tilde{V}\right)^{-2}\left[2.409-3.033\left(y\tilde{V}\right)^{-2}\right]+\left[2^{-1/6}y\left(y\tilde{V}\right)^{-1/3}-(1/3)\right]\left[1-2^{-1/6}y\left(y\tilde{V}\right)^{-1/3}\right]^{-1} \quad (3b)$$

In Eqns (3a) and (3b) the reduced thermodynamic coordinates $\tilde{T}$ and $\tilde{V}$ appear; in this way, the equation is independent of the particular structure:

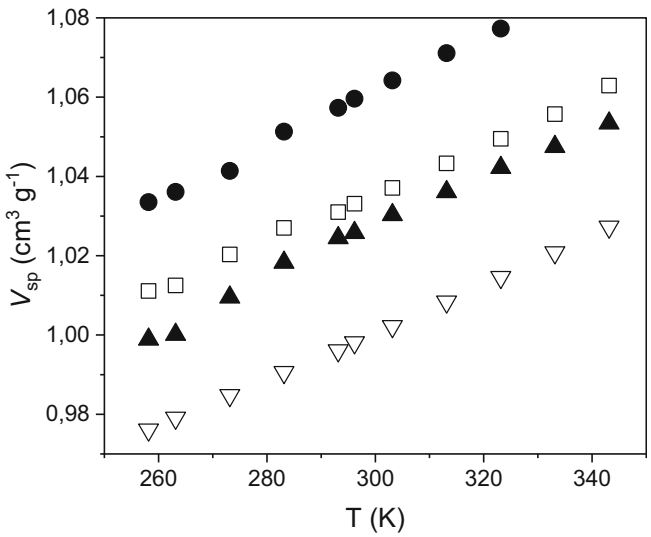

Figure 3. Specific volume V_{sp} as a function of temperature T for the investigated elastomers (R1, circles; R2, squares; R3, down triangles; R4, up triangles). Uncertainties are within the size of the data points.

Table 2. Scaled thermodynamic parameters T^* and V^* for the investigated samples. Uncertainties are less than 1% for both parameters

Sample	T^* (K)	V^* (cm^3 g^{-1})
R1	9755	1.0171
R2	10 339	1.0215
R3	10 230	0.9762
R4	9853	0.9879

$$\tilde{T}=T/T^*;\ \tilde{V}=V/V^*$$

Parameters T^* and V^*, essential to apply the equation to a specific elastomer, can be obtained from a fitting procedure of Eqns (3a) and (3b) to the data shown in Fig. 3. However, in this study we used a simpler interpolation expression[30]:

$$\ln\frac{V}{V^*}=A+B\left(\frac{T}{T^*}\right)^{3/2}$$

($A=-0.10346$, $B=23.854$). Indeed, the two procedures produce almost identical results, at atmospheric pressure.[30] The values of the scaled parameters for the investigated elastomers are presented in Table 2.

In Eqns (3a) and (3b), y represents the volume fraction of occupied sites; consequently, $h=1-y$ plays the role of the calculated free volume fraction. Parameter y does depend on temperature, due to the presence of the interstitial free volumes, although the expansion coefficient is of the order of 10^{-5} K^{-1} for most polymers.[31] Figure 4 shows as an example the behaviour of the specific and the occupied volume for sample R1 *versus* temperature.

The specific free volume, V_f, is given by:

$$V_f=V_{sp}-V_{occ}=Nv_h \quad (4)$$

where V_{occ} is defined in terms of the van der Waals volume and the interstitial free volume[32]: $V_{occ}=V_{VdW}+V_{if}$. In fact, interstitial free volume consists of local empty spaces too minute to localize

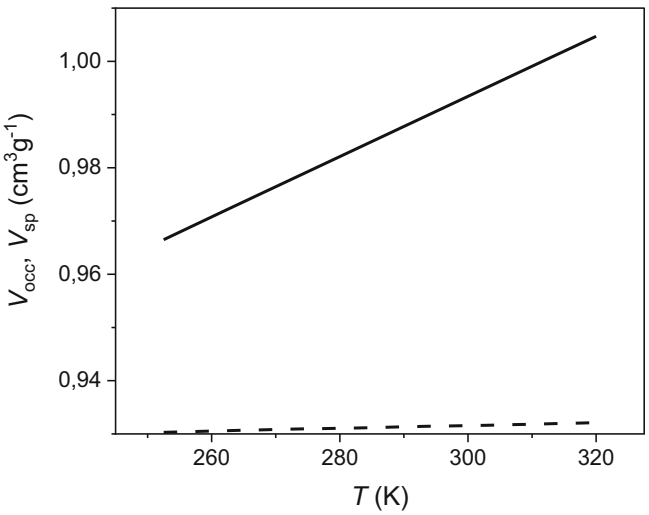

Figure 4. Dependence of occupied volume (dashed line, as obtained from the Simha–Somcynsky theory) and specific volume (continuous line) for R1 *versus* temperature. Their difference is the excess free volume (the free volume deducted from the interstitial free volume).

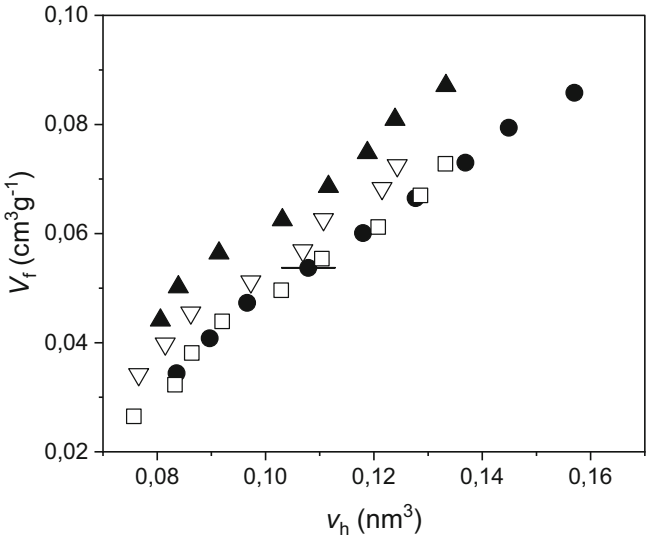

Figure 5. V_f *versus* v_h, using spherical approximation for holes (R1, circles; R2, squares; R3, down triangles; R4, up triangles). Uncertainties for V_f are within the size of the data points; for v_h uncertainty is shown for a single data point for the sake of clarity.

even a small probe such as Ps and it is associated with the occupied volume. The dependence of the occupied volume on the temperature is ascribed to the expansion of such interstitial free volumes and is incorporated in the lattice-hole model.[32]

A plot of the difference V_f between the specific volume (as obtained from dilatometry) and specific occupied volume (from the theory) *versus* the hole volume should give the number density of holes, N. If this last is constant in the explored range of temperatures, the plot should be fitted by a straight line. Figure 5 shows such plots for the investigated elastomers; holes are approximated by spheres. The linear trend (correlation coefficient > 0.99) obtained for the various samples guarantees that N is constant. The values found are presented in Table 3.

Finally, we can apply Eqn (1) to evaluate the free volume fraction for the investigated elastomers and compare it to the theoretical prediction. The results are shown in Fig. 6. We point out that the free volume fraction obtained from a combination of PALS and dilatometry is not a 'pure' experimental result, since it depends on the geometry chosen for the holes, implicit in v_h.

DISCUSSION

Figure 6 points out a systematic difference between f and h for spherical holes, which remains even by changing the hole geometry. With, for example, a cuboidal geometry we can mitigate the discrepancy but we cannot get a satisfactory fit. Therefore, we allowed the cavities to expand preferentially in some directions with increasing temperature. In order to obtain a simple model, we adopted a cylindrical shape, for which the relationship between o-Ps lifetime and hole radius is known,[33,34] but with a non-constant aspect ratio q of the cylinder, since we suppose that the radius can expand at a different rate with respect to the height of the cylinder. Without going into details, which can be found elsewhere,[21] we assume that the relationship between height s and radius r of the cavity follows a power law:

$$\frac{s}{s_0} = \left(\frac{r}{r_0}\right)^p$$

where s_0 and $r_0 = q_0 s_0$ are height and radius at a given temperature; q_0 is the corresponding aspect ratio. The exponent p is an index of anisotropic growth. Clearly, $p = 1$ means a cylinder expanding in an isotropic way with temperature. It is straightforward to obtain the radius from the o-Ps lifetime for such a cavity and the hole volume for each temperature; then, by considering q_0 and p as free parameters, we used the same procedure adopted for spherical holes (that is, plot of V_f *versus* v_h to obtain the value of N, calculation of f using Eqns (3a) and (3b) and quantitative comparison with h by means of a statistical test) in order to obtain the best fit. It turns out that only flattened cavities ($q < 1$) produce a satisfactory agreement between f and h; elongated holes do not give good fits, for any of the investigated elastomers. The results are shown in Fig. 6; Table 4 reports the values of parameters q_0 and p.

Since it is a two-parameter fit, the uncertainty associated with each parameter is quite high, about 20% for p and 25% for q_0. Nevertheless, the anisotropic expansion of the cavities is evident from the low value of p, as well as a flattened morphology ($q_0 < 1$), even though the present one is a simplified model of an irregular hole.

In the range of investigated temperatures, the cavity radius scales linearly with temperature. Table 4 reports the hole radius extrapolated at the glass transition. The values found are in the range 2.9–3.6 Å. Therefore, the diameter of a hole is comparable to the effective bond length l, defined as the square root of the ratio between the unperturbed mean-square end-to-end distance $\langle R^2 \rangle_0$ of a chain and the number of its backbone bonds, which is equal to 5 ± 2 Å, as estimated by Wang.[35] Milner[36] reported a comparable value (6 Å). Similar results were also obtained for a fluoroelastomer and for a *cis*-polyisoprene rubber.[20] It is remarkable that a typical size of holes at the glass transition for different elastomers matches quite well to l, a parameter related to reptation motions and largely independent of the macromolecular structure.

The values of the number density N of holes (Table 4) are similar to those obtained using the spherical approximation (Table 3).

From Table 4 we also observe that the value of parameter p is almost independent of the content of acrylonitrile of the copolymers R1–R3. It is identical, within errors, to the value found[21] for the homopolymer polybutadiene, that is, 0.28. We can deduce that the presence of acrylonitrile, which increases from one unit every four units of butadiene in R1 to a ratio of almost unity in R3, does not influence significantly the expansion features of the holes. This result is different from that found in polybutadiene–polyisoprene blends,[21] where an increase of the volume fraction of polyisoprene, from 0 to 100%, was linearly correlated to an increase of p, from 0.28 to 0.78 (correlation coefficient of 0.91), as shown in Fig. 7, built from previously reported data.[21]

If the increased presence of isoprene seems to make the hole expansion more isotropic, on the contrary the presence of

Table 3. Number density of holes N for the investigated elastomers. Holes are approximated by spheres

	R1	R2	R3	R4
N (10^{21} g^{-1})	0.69	0.76	0.75	0.92

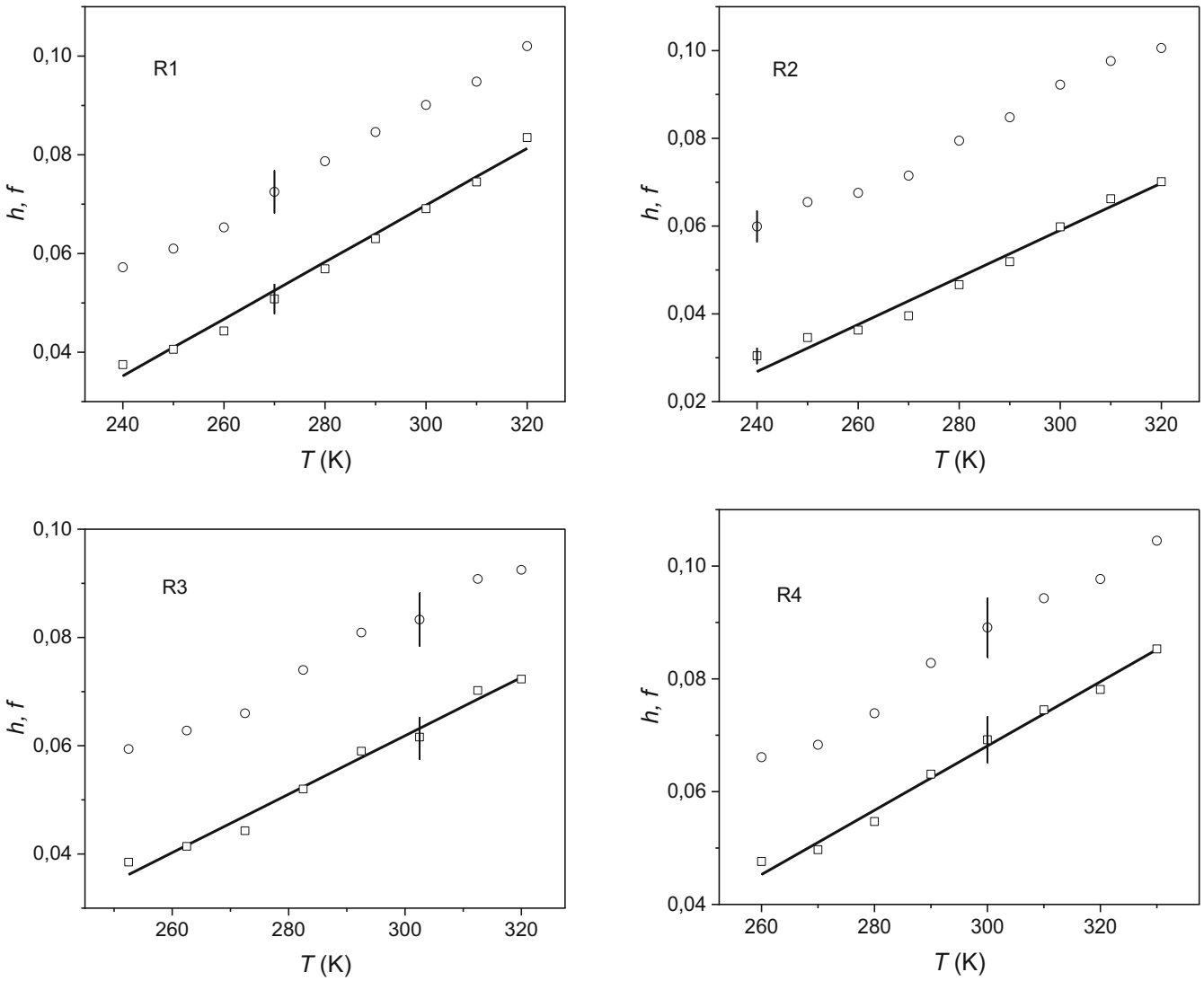

Figure 6. Free volume fraction *f* as determined from PALS and dilatometry *versus* temperature for the four elastomers, compared with the free volume fraction *h* (continuous line), as obtained from the Simha–Somcynsky equation (circles, spherical holes; squares, anisotropic holes).

acrylonitrile does not influence such feature. In this connection, it is worth observing that R4, a terpolymer with identical percentages of butadiene, isoprene and acrylonitrile, shows a value of *p* which is very similar to the average of the values ascribable to the presence of each component.

The presence of acrylonitrile seems to be correlated to an increase of the aspect ratio q_0, which acquires higher values, between 0.4 and 0.5, for the copolymers here investigated, with respect to the butadiene–isoprene blends.

Table 4. Parameters for the investigated elastomers resulting from a fitting procedure. The radius of the hole at T_g is also shown

	R1	R2	R3	R4
q_0	0.43	0.45	0.50	0.50
p	0.26	0.25	0.28	0.46
N (10^{21} g^{-1})	0.64	0.49	0.64	0.77
r (T_g) (Å)	2.9	3.6	3.5	3.3

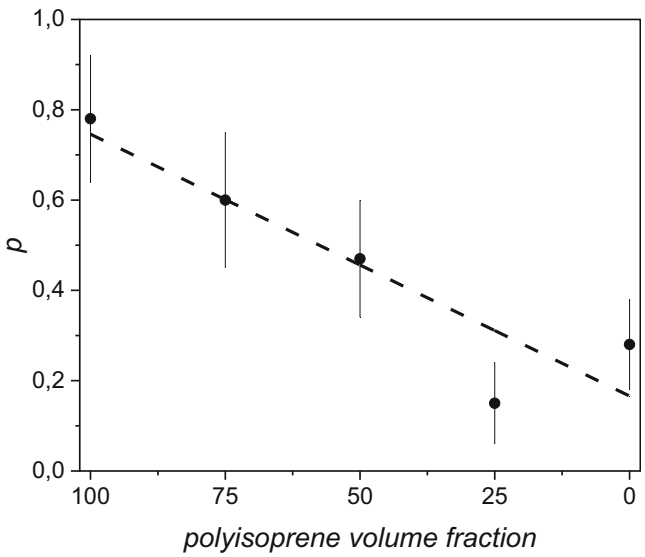

Figure 7. Behaviour of parameter *p* *versus* polyisoprene volume fraction in polybutadiene–polyisoprene blends (data taken from Consolati *et al.*[21]).

The model here proposed of preferential hole growth in some directions is rather simple, since it does not consider that the constraints can be temperature-dependent; in this connection, parameter p could be expected to change with temperature. To unravel such a possible dependence, data with much higher statistics would be needed. Nevertheless, the model is compatible with the dynamics of macromolecules whose motions can be subjected to physical (e.g. entanglements) or chemical (e.g. crosslinks) constraints and can be applied to any amorphous polymer at equilibrium.

Finally, we remark that our approach to evaluate the free volume fraction differs from the usual assumption of a linear relation between the number density of holes N and o-Ps intensity I_3. In this case f is written as:

$$f = Cv_h I_3 \tag{5}$$

the constant C being dependent on the polymer structure. We have doubt that Eqn (5) correctly describes the free volume fraction. Indeed, it has been remarked[37,38] that various factors influence Ps formation and so I_3; therefore, it is generally not possible to disentangle the contribution of the number density of holes. In particular, measurements of poly(methyl methacrylate) (PMMA) samples[38] over a wide range of temperatures showed that o-Ps intensity displays hysteresis; the effect has been attributed to processes of radiation chemistry in the terminal track of the positron, and in this case I_3 does not reflect simply the variation in the number density of holes with temperature. Furthermore, increase of I_3 was observed in γ-irradiated polyethylene and PMMA6N (PMMA containing 6% of methyl acrylate) at low temperature[39]; the effect has been attributed to additional Ps formation on trapped electrons generated by irradiation. Quantitative analysis of the phenomenon[40] strongly supports the conclusion that I_3 is mainly dependent on the probability of Ps formation and not simply on the number density of free volume holes, since all o-Ps atoms are trapped before annihilation. According to the spur model,[41] positrons produce electrons during their slowing down; Ps is formed by interaction of the positron with one of the electrons created in the terminal track. As a consequence, no Ps is formed in the lack of the spur electrons, even in the presence of a high number of free volume holes. If we further consider that the presence of positron acceptors (e.g. carbonyl groups) is also influencing I_3, we see that this parameter is the result of various complicated and interrelated processes.[42] For these reasons we preferred to follow the alternative approach of Shritawatpong *et al.*[19]

CONCLUSIONS

In this work we studied the expansion of the free volume in three polybutadiene–acrylonitrile rubber copolymers and in a polybutadiene–polyisoprene–acrylonitrile terpolymer, above the glass transition in order to compare the experimental results with the lattice-hole model. Analysis of the results from two techniques, dilatometry and PALS, allowed us to correlate the expansion of the sub-nanometric cavities forming the free volume with the dependence of the specific volume on temperature. An analytical treatment forces one to model the holes, in fact irregular, through simple geometries. It follows that the description of the holes is necessarily rather rough; nevertheless, it is important to distinguish, among the various approximations, the most suitable one to get insight into the hole morphology.

The choice of the hole shape influences also the evaluation of the free volume fraction, according to our discussion.

Comparison with the theory allowed us to conclude that, on the one hand, spherical cavities produce a free volume fraction systematically higher than predicted. On the other hand, cylindrical flattened holes with preferential expansion in the radial direction with respect to the axial one give a very good agreement. The presence of acrylonitrile does not influence the way the cavities expand, differently with respect to polybutadiene–polyisoprene blends,[21] where parameter p – quantifying the anisotropy growth – scales linearly with polyisoprene volume fraction of the blend and can be predicted by the p values of the homopolymers. This conclusion is strengthened by the fact that the value of p for terpolymer R4 is equal, within errors, to what could be expected by taking an average of values of the parameter for each component.

We have also found that the values of the radius of the hole, extrapolated at T_g, agree with the estimated value of the effective bond length, which is predicted to be rather constant and independent of polymer chemical structure on passing from the glassy to the equilibrium state.

Finally, we point out the importance of dilatometry, since it allows one not only to obtain the scaled thermodynamic parameters essential to apply the Simha–Somcynsky equation of state to our particular elastomers, but also to get the number density of holes without referring to the o-Ps intensity.

ACKNOWLEDGEMENTS

Open Access Funding provided by Politecnico di Milano within the CRUI-CARE Agreement.

REFERENCES

1 Batshinski AJ, *Z Phys Chem* **84**:643 (1913).
2 Fox TG and Flory PJ, *J Appl Phys* **21**:581–591 (1950).
3 Doolittle AK, *J Appl Phys* **22**:1031–1035 (1951).
4 Ryong-Joon R, MD simulation study of glass transition and short time dynamics in polymer liquids, in *Atomistic Modeling of Physical Properties*, Vol. **116**, ed. by Monnerie L and Suter UW. Springer, Berlin, pp. 111–144 (1994).
5 Bondi A, *J Phys Chem* **58**:929–939 (1954).
6 Hedenqvist M, Angelstok A, Edsberg L, Larsson P and Gedde U, *Polymer* **37**:2887–2902 (1996).
7 McGonigle E-A, Liggat JJ, Pethrick RA, Jenkins SD, Daly HJ and Hayward D, *Polymer* **42**:2413–2426 (2001).
8 Simha R and Somcynsky T, *Macromolecules* **2**:342–350 (1969).
9 Rodgers PA, *J Appl Polym Sci* **48**:1061–1080 (1993).
10 Swapna VP, Nambissan PMG, Thomas SP, Kaliyathan AV, Jose T, George SC *et al.*, *Polym Int* **68**:1280–1291 (2019).
11 Chaos A, Sangroniz A, Gonzalez A, Iriarte M, Sarasua JR, del Rio J *et al.*, *Polym Int* **68**:125–133 (2019).
12 Wu J-w, Huang Y, Li H-B, Runt J and Yeh J-T, *Polym Int* **67**:454–462 (2018).
13 Prasad K, Nikzad M, Doherty CM and Sbarski I, *Polym Int* **67**:717–725 (2018).
14 Berko S and Pendleton HN, *Annu Rev Nucl Part Sci* **30**:543–581 (1980).
15 Don H and Jacob KI, *Macromolecules* **36**:8881–8885 (2003).
16 Račko D, Capponi S, Alvarez F, Colmenero J and Bartoš J, *J Chem Phys* **131**:064903 (2009).
17 Hofmann D, Entrialgo-Castano M, Lerbret A, Heuchel M and Yampolskii Y, *Macromolecules* **36**:8528–8538 (2003).
18 Consolati G, *J Chem Phys* **117**:7279–7283 (2002).
19 Srithawatpong R, Peng ZL, Olson BG, Jamieson AM, Simha R, McGervey JD *et al.*, *J Polym Sci B: Polym Phys* **37**:2754–2770 (1999).
20 Consolati G, Nichetti D, Briatico Vangosa F and Quasso F, *Rubber Chem Technol* **92**:709–721 (2019).
21 Consolati G, Mossini E, Nichetti D, Quasso F, Viola GM and Yainik E, *Int J Mol Sci* **22**:1436 (2021).
22 Utracki L, *J Polym Sci B: Polym Phys* **45**:270–285 (2007).

23 Limper A, *Mixing of Rubber Compounds*. Hanser Fachbuchverlag, Munich, Germany (2012).
24 Kansy J, *Nucl Instrum Methods Phys Res A* **374**:235–244 (1996).
25 Plotkowski K, Panek TJ and Kansy J, *Il Nuovo Cimento D* **8**:933–940 (1988).
26 Consolati G, Panzarasa G and Quasso F, *Polym Test* **68**:208–212 (2018).
27 Tao SJ, *J Chem Phys* **56**:5499–5510 (1972).
28 Eldrup M, Lightbody D and Sherwood N, *Chem Phys* **63**:51–58 (1981).
29 Nakanishi H, Wang SJ and Jean YC, Microscopic surface tension studied by positron annihilation, in *Positron Annihilation Studies of Fluids*, ed. by Sharma SC. World Scientific, Singapore, pp. 292–298 (1988).
30 Utracki LA and Simha R, *Macromol Theory Simul* **10**:17–24 (2001).
31 Simha R and Wilson PS, *Macromolecules* **6**:908–914 (1973).
32 Dlubek G, Local free-volume distribution from PALS and dynamics of polymers, in *Polymer Physics: From Suspensions to Nanocomposites and Beyond*, ed. by Utracki LA and Jamieson AM. John Wiley & Sons, Singapore, pp. 421–472 (2010).
33 Jasinska B, Koziol AE and Goworek T, *J Radioanal Nucl Chem* **210**:617–623 (1996).
34 Olson BG, Prodpran T, Jamieson AM and Nazarenko S, *Polymer* **43**: 6775–6784 (2002).
35 Wang SQ, *Macromolecules* **40**:8684–8694 (2007).
36 Milner ST, *Macromolecules* **38**:4929–4939 (2005).
37 Shantarovich VP, *J Radioanal Nucl Chem* **210**:357–369 (1996).
38 Wang CL, Hirade T, Maurer FJH, Eldrup M and Pedersen NJ, *J Chem Phys* **108**:4654–4661 (1998).
39 Hirade T, Maurer FJH and Eldrup M, *Radiat Phys Chem* **58**:165–471 (2000).
40 Shantavovich VP, Hirade T, Kevdina IB, Gustov VW and Oleinik EF, *Acta Phys Pol A* **99**:497–501 (2001).
41 Mogensen OE, in *Positron Annihilation in Chemistry*, ed. by Goldanskii VI. Springer-Verlag, Berlin (1995).
42 Shantarovich VP, *J Polym Sci B: Polym Phys* **46**:2485–2503 (2008).

